Engineering Innovations
ISSN: 2813-1002, Vol. 14, pp 1-13
doi:10.4028/p-V2Z9mr

Submitted: 2025-01-11
Revised: 2025-03-11
Accepted: 2025-03-12
Online: 2025-04-04

Tunable Hydrophobicity and Photoluminescence in Polystyrene-Calcium Carbonate Composites with Citric Acid-Induced Porosity

Ayodunmomi Esther Olowofoyeku[1,a*], Ademola Kabiru Aremu[2,b], Abel Olajide Olorunnisola[3,c], Ayobamiji Emmanuel Olowofoyeku[4,d], Jesus Roberto Villegas Mendez[5,e], Daniel Gbenga Adekanmi[5,f]

[1]Pan African University Life and Earth Sciences Institute (Including Health and Agriculture), PAULESI, University of Ibadan, Ibadan, Nigeria

[2]Department of Agriculture and Environmental Engineering, University of Ibadan, Ibadan, Nigeria

[3]Department of Wood Products Engineering, University of Ibadan, Ibadan, Nigeria

[4]Faculty of Chemical Science, Olusegun Agagu University of Science and Technology, Ondo, Nigeria

[5]Facultad de Ciencias Químicas, Universidad Autónoma de Coahuila, Saltillo, Coahuila, 25280, México

[a]ayoolowo1122@gmail.com, [b]ademolaomooroye@gmail.com, [c]abelolorunnisola@yahoo.com, [d]banjiolowo1@gmail.com, [e]jesus.villegas@uadec.edu.mx, [f]danieladekanmi@uadec.edu.mx

Keywords: photoluminescence, porous composites, calcium carbonate, oleic acid, citric acid, surface modification, adsorption, polystyrene.

Abstract. Polystyrene (PS) is widely used in industries like packaging and insulation, with calcium carbonate often incorporated as a filler to enhance mechanical properties. However, its potential in tuning surface and optical properties remains unexplored. This study addresses this gap by investigating the effects of dual modification, oleic acid for surface hydrophobicity and citric acid for controlled porosity, on PS-calcium carbonate composites. Calcium carbonate was surface-modified with oleic acid, and PS-calcium carbonate composites (40:60 weight ratio) were synthesized using the melt blending method, followed by citric acid treatment of the composites that resulted in up to 8.90% weight loss in NPS3. X-ray diffraction (XRD) and Fourier transform infrared transform FTIR analyses confirmed no chemical interaction between phases but revealed partial dissolution of calcium carbonate due to citric acid treatment. Contact angle measurements showed increased hydrophilicity after citric acid treatment, while oleic acid imparted hydrophobicity, with NPS3 and TPS3 exhibiting higher contact angles than NPS2 and TPS2. SEM images revealed matrix cavities (up to 50 μm wide), especially in TPS3. Hardness testing showed a decrease in hardness with increasing oleic acid concentration, with TPS3 exhibiting the lowest value (60.7 Shore D). Photoluminescence measurements revealed broad emission spectra with a blue shift at lower oleic acid concentrations, while higher concentrations caused a red shift and broader emission, stabilized by citric acid treatment. Solvent absorption tests indicated enhanced absorption, with TPS3 absorbing 33.10% vegetable oil and 20.80% of both hexane and diesel respectively. Overall, these modifications significantly tuned the composites' mechanical, morphological, and optical properties, demonstrating potential for sensing applications.

Introduction

The development of advanced materials to meet the growing demands of modern industries has driven significant innovation in polymer composite design. Among polymers, polystyrene (PS) is widely utilized due to its affordability, versatility, and ease of processing, with applications spanning packaging, insulation, and engineering components. However, its inherent brittleness, limited impact resistance, and environmental persistence restrict its utility in high-performance and sustainable systems [1]. Addressing these challenges requires novel approaches that integrate innovative filler systems to enhance mechanical, thermal, and functional properties while improving environmental sustainability [2-4].

Fillers play a pivotal role in defining the properties of polymer composites. Calcium carbonate, an abundant and cost-effective mineral, is a popular material for reinforcing polymer matrices. Its benefits include enhanced stiffness, thermal stability, and reduced shrinkage during polymer processing, all achieved while adhering to green chemistry principles by minimizing reliance on energy-intensive or environmentally harmful additives [5, 6]. PS-calcium carbonate composites offer a versatile platform for addressing industry-specific requirements. Research demonstrates that calcium carbonate improves tensile strength, flexural properties, and thermal stability in various polymer systems, including PS [7, 8]. However, incorporating untreated calcium carbonate into hydrophobic polymers like PS presents compatibility issues, such as poor dispersion and weak interfacial bonding, which hinder composite performance [9-11].

Surface modification of calcium carbonate is used to address polymer-filler compatibility challenges. The use of fatty acids like stearic and oleic acid as surface modifiers effectively imparts hydrophobicity to the calcium carbonate surface, promoting uniform dispersion within the polymer matrix and stronger interfacial adhesion [9, 12]. Many studies have shown the effectiveness of oleic acid as a surface modifier for enhancing hydrophobicity. For example, Dweiri et al. used it to modify calcium carbonate [13], while Wang et al. applied it to carbon nanotubes [14]. while Wang et al. applied it to carbon nanotubes [15], and Kawamura et al. used it for magnetic nanomaterials [16]. Surface modification of fillers also influences the mechanical toughness, elasticity, and processability of composites. It minimizes filler aggregation, promotes uniform stress distribution, and improves the structural integrity of the material [12]. While Fatty acids are commonly employed as surface modifiers to enhance compatibility in composites, strong acids are used to treat polymers, introducing hydrophilic functional groups that significantly increase their hydrophilicity [17].

Polymers are typically not inherently photoluminescent, but incorporating materials like carbon dots or rare-earth luminescent particles transforms them into versatile composites with enhanced optical properties. This integration expands their functionality, enabling applications in advanced optical systems, solid-state lighting, display technologies, and sensors for detecting physical and biochemical parameters through luminescent responses. However, many conventional luminescent agents are expensive, require complex processing, or pose environmental risks due to rare-earth metal accumulation [18-21].

This study explores how oleic acid modification and subsequent citric acid treatment influence the tunability of structural, morphological, and photoluminescent properties in PS-calcium carbonate composites. The composites, synthesized via melt blending, were characterized using XRD for structure, SEM for morphology, and Shore hardness testing. The research further investigated the synergistic effects of oleic acid-modified calcium carbonate and citric acid-induced porosity on the composites' hydrophobicity, optical properties, and solvent adsorption for a better understanding of their potential for sustainable, high-performance applications.

Materials and Methods

Materials

The materials used in this study include industrial-grade calcium carbonate (particle size: 10 μm, 98% purity), pure polystyrene (PS) pellets (melt flow rate: 5 g/10 min, 99.5% purity), oleic acid (99% purity), citric acid (99% purity), ethanol (96% v/v), and distilled water. All chemicals were sourced from reputable suppliers and used without additional purification.

Surface Modification of Calcium Carbonate with Oleic Acid

Calcium carbonate was modified by oleic acid at varying concentrations (0%, 0.75%, and 2.50 % by weight). Oleic acid was dissolved in 100 mL of ethanol, and 100 g of calcium carbonate was added to this solution. The mixture was stirred continuously for 3 h at room temperature to ensure efficient adsorption of the oleic acid onto the calcium carbonate surface. Thereafter, the ethanol was evaporated at 70 °C while stirring for an additional 3 h to prevent particle agglomeration. The modified carbonates were ground and labeled based on the oleic acid concentration: C1 (0 % oleic

acid), C2 (0.75 % oleic acid), and C3 (2.50 % oleic acid), and then they were stored for subsequent composite preparation [22]. Wettability was assessed using a sessile drop contact angle test on a Drop Shape Analyzer (DSA30, Krüss). The contact angle was measured to quantify surface hydrophobicity, with higher angles indicating increased water repellency.

Preparation of PS-Calcium Carbonate Composites

The PS-calcium carbonate composites were fabricated by melt blending 60 wt% modified calcium carbonate with 40 wt% pure PS using a twin-screw extruder. Processing was conducted at 120 °C with a screw speed of 120 rpm for 10 minutes. The resulting extrudates were pressed into films and cut into standard test pieces. The composites were designated as NPS1, NPS2, and NPS3, based on the oleic acid-modified Calcium carbonate content. A control sample, comprising pure PS without Calcium carbonate, was processed under identical conditions and labeled as NPS [23]. The wettability of the samples was also assessed using a sessile drop contact angle test.

Citric Acid Treatment of the Materials

Each sample (NPS, NPS1, NPS2, and NPS3) was treated with 50 mL of 1 M citric acid solution for 48 h, followed by thorough rinsing with distilled water to remove residual acid. The samples were then dried at 35 °C for 12 h. The citric acid-treated composites were designated as TPS1, TPS2, and TPS3, while the treated pure PS was labeled as TPS. The weight loss due to citric acid treatment was calculated using Equation 1:

$$\text{Weight loss } (\%) = \frac{W_1 - W_0}{W_0} \times 100 \quad (1)$$

where W_0 and W_1 represent the initial and final weights of the samples, respectively.

Structure of the Composites

X-ray diffraction (XRD) analysis was performed to examine the crystallographic structures of calcium carbonate and its composites. XRD patterns were recorded using a Malvern Panalytical Empyrean X-ray diffractometer with Cu Kα radiation (λ=1.5406 Å) over a 2θ range of 10° to 70°.

Morphology of the Composites

The morphology of the samples was analyzed using scanning electron microscopy (SEM) with a JEOL JSM 6610LV at 600x magnification. The attached Energy Dispersive X-ray Spectroscopy (EDS) was employed to assess the elemental composition, while surface roughness profiles were analyzed using Gwyddion software.

Functional Groups

Fourier transform infrared (FTIR) spectroscopy was used to examine the chemical interactions between PS, calcium carbonate, and the surface-modifying agents. Spectra were recorded using a PerkinElmer Spectrum Two FTIR spectrometer in the range of 4000 – 600 cm^{-1} with the Attenuated Total Reflectance (ATR) method, providing insights into the functional groups and chemical bonding within the composites.

Photoluminescence Spectroscopy

The photoluminescence (PL) properties of the composites were measured using a Shimadzu RF-6000 spectrofluorophotometer, with excitation at wavelengths of 255 nm and 405 nm. Furthermore, NPS3 and TPS3 samples were subjected to 10 cycles of UV irradiation at 255 nm for 5 minutes, followed by 1 h of darkness, as described by Abd El-Lateef et al. [24]. The emission peak intensity following each cycle was quantified as a percentage of their initial intensity to assess the stability of photoluminescence.

Shore Hardness

The hardness of the PS-calcium carbonate composites was evaluated using a Shore D durometer following ASTM D2240 standards. Samples (50 mm × 50 mm × 2 mm) were tested at three random locations, and the average hardness value was recorded to assess the mechanical strength of the composites.

Solvent Absorption Capacity

The solvent absorption capacity of the composites was evaluated by immersing 100 mm x 100 mm x 2 mm samples in various solvents (water, vegetable oil, n-hexane, and diesel) for 24 h. After immersion, the samples were removed, gently cleaned, and weighed to determine the change in mass. The absorption capacity was calculated using Equation 2:

$$\text{Absorption Capacity (\%)} = \frac{W_1 - W_0}{W_0} \times 100 \quad (2)$$

where W_0 and W_1 represent the initial and final weights of the samples, respectively.

Statistical Analysis

Experiments were carried out in triplicate, and the results are reported as mean values with their corresponding standard deviations. Statistical significance was evaluated using analysis of variance (ANOVA), complemented by Dunnett's multiple comparison test ($p < 0.05$). All statistical analyses were performed using GraphPad Prism 8 software.

Results and Discussion

Effect of Oleic Acid Treatment on the Wettability of Carbonate Fillers

Fatty acid treatments, like oleic acid modification, are used to increase the hydrophobicity of fillers like calcium carbonate. This improves their dispersion in polymer matrices and reduces moisture absorption by altering the surface energy [25-27]. Fig. 1 shows the contact angle results of calcium carbonate treated with various oleic acid concentrations. While moderate oleic acid improved dispersion, excessive concentrations, as seen in C3 with a contact angle of 170.70°, cause agglomeration. The stronger hydrophobic interactions between particles led to clumping, which disrupted uniformity and reduced performance in the polymer matrix [28].

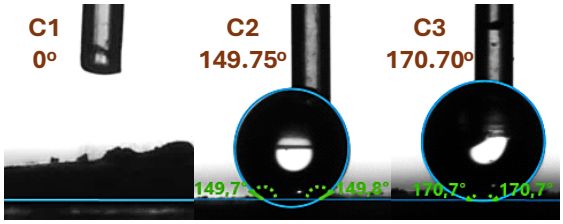

Fig. 1. Contact angles of the oleic acid-treated calcium carbonate.

Citric Acid Treatment and Wettability of the Composites

As shown in Table 1, negligible weight loss was observed in pure PS (NPS), indicating minimal structural impact. In contrast, composites (NPS1, NPS2, and NPS3) exhibited significantly higher weight losses ($P < 0.0001$), attributed to the increased porosity induced by citric acid treatment. These changes align with surface morphology modifications, highlighting the composites' responsiveness to treatments and adsorption processes. Contact angle measurements (Fig. 2) further confirm the effect of citric acid treatment, with citric acid treated composites showing reduced contact angles and increased hydrophilicity. NPS3 and TPS3 exhibited higher contact angles than NPS2 and TPS2, respectively, emphasizing the hydrophobic nature imparted by the oleic acid compared to NPS1 and TPS1. While oleic acid introduces hydrophobicity, citric acid treatment remains the dominant factor in enhancing surface hydrophilicity.

Table 1. Filler composition and sample weight loss after citric acid treatment.

Sample	Filler	Filler Oleic Acid treatment (wt%)	Filler-to-Polystyrene ratio	Weight Loss after citric acid treatment (%)	Equivalent citric acid-treated sample
NPS	--	--	0:100	0.01 ± 0.01	TPS
NPS1	C1	0.00	60:40	9.81 ± 0.34	TPS1
NPS2	C2	0.75	60:40	9.75 ± 0.20	TPS2
NPS3	C3	2.50	60:40	8.90 ± 0.25	TPS3

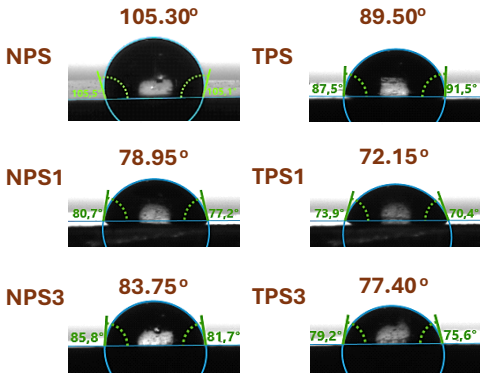

Fig. 2. Contact angles of the PS-calcium carbonate composites.

Structural Analysis

The crystalline and amorphous characteristics of calcium carbonate fillers, PS, and their composites, as analyzed through x-ray diffraction, are shown in Fig. 3a and 3b. The diffraction patterns of modified calcium carbonate (Fig. 3a) matched ICDD card 01-070-0095, confirming a monoclinic crystalline structure with prominent peaks at 2θ = 29.73° (104), 36.31° (110), 39.81° (113), and 43.57° (202) as has been reported in other studies [22]. In C2 and C3, oleic acid treatment reduced the intensity of these peaks due to lattice disruption and the formation of a hydrophobic coating, as also reported by similar studies [22, 29]. PS, including both untreated (NPS) and citric acid-treated (TPS), displayed its characteristic amorphous hump around 2θ = 19°, confirming its non-crystalline nature [30, 31].

The XRD patterns of PS-calcium carbonate composites (Fig. 3b) combined crystalline peaks from calcium carbonate with the amorphous hump of PS showing no chemical bonding evidence in the composites (NPS1, NPS2, NPS3), carbonate peaks dominated due to the higher intensity of the crystalline phase, overshadowing the amorphous PS peak. In citric acid-treated composites (TPS1, TPS2, TPS3), the calcium carbonate diffraction intensity decreased, attributed to its partial dissolution. The more pronounced PS hump in the citric acid-treated composites indicates that the polymer's structure remained intact after the treatment. Additionally, TPS3 exhibited stronger calcium carbonate peaks than TPS1, due to a higher surface coating of oleic acid in C3.

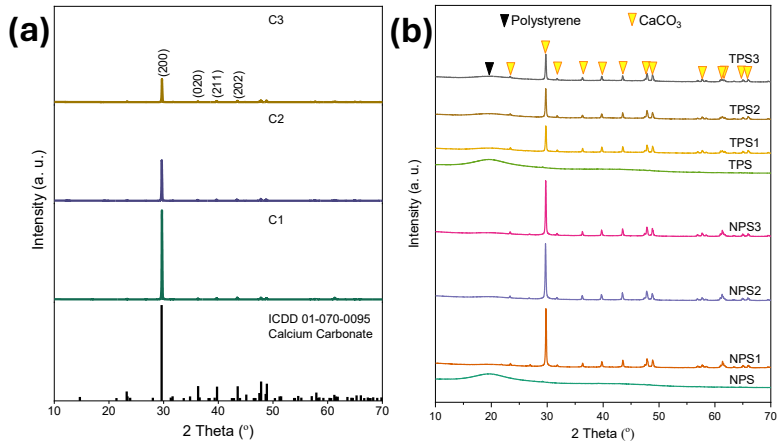

Fig. 3. XRD spectra of (a) oleic acid-treated calcium carbonate and (b) PS-calcium carbonate composites.

Functional Groups

The Fourier transform infrared (FTIR) spectra presented in Fig. 4a and 4b confirmed the functional groups present in calcium carbonate, PS, and their composites. Calcium carbonate (C1) exhibited characteristic peaks at 1395, 1080, and 875 cm^{-1}, corresponding to the carbonate anion's asymmetric stretching, symmetric stretching, and out-of-plane bending vibrations, respectively [22, 28, 32]. Surface modification with oleic acid in C2 and C3 intensified the 1395 cm^{-1} peak and introduced new peaks around 2850 – 2920 cm^{-1}, representing alkyl chains from oleic acid [22]. Pure PS (NPS) displayed aromatic absorption bands, including C-H stretching at 3020 cm^{-1}, aliphatic C-H stretch around 2900 cm^{-1}, aromatic ring stretching at 1600 cm^{-1}, and out-of-plane bending near 700 cm^{-1} [33]. These peaks persisted in treated PS (TPS), with a slight increase in intensity in the 700 cm^{-1} region, suggesting enhanced surface activity due to acid treatment [17]. In untreated composites (NPS1, NPS2, NPS3), the absorption bands of PS and calcium carbonate overlapped. The carbonate peak at 1600 cm^{-1} merged with the aromatic ring stretch, while the 875 cm^{-1} peak remained prominent, indicating the coexistence of the polymer matrix and filler. These overlaps, along with the absence of new peaks, confirm interfacial interactions rather than chemical bonding [34]. Citric acid-treated composites (TPS1, TPS2, TPS3) showed reduced intensities in carbonate peaks at 1395 and 875 cm^{-1}, reflecting the partial dissolution of calcium carbonate.

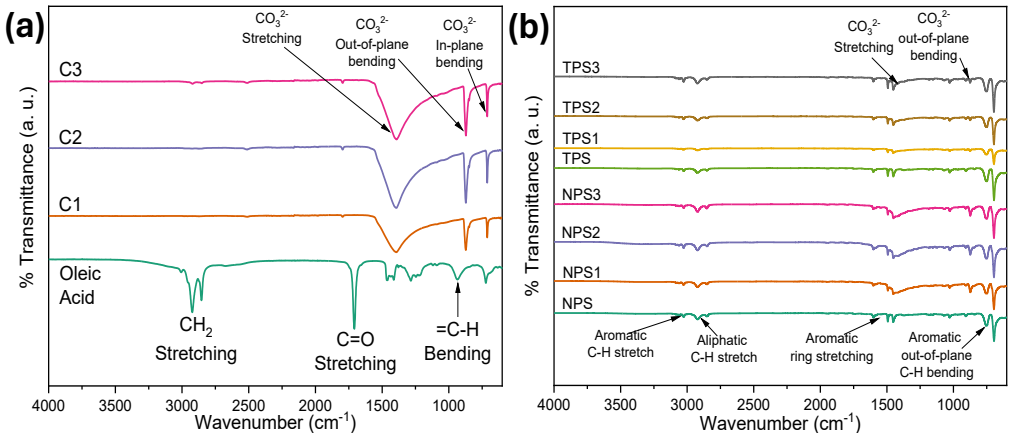

Fig. 4. FTIR spectra of (a) oleic acid-treated calcium carbonate, and (b) PS-calcium carbonate composites.

Surface Morphology and Roughness Characteristics

The SEM micrographs in Fig. 5a show the morphological changes before and after citric acid treatment. Pure PS (NPS) has a smooth surface, which remains largely unchanged after treatment (TPS), with only minor indentations likely due to surface artifacts similar to other studies [24]. In the composites, the addition of calcium carbonate introduced particles of varying sizes, up to 50 μm, dispersed throughout the polymer matrix. However, composites made with oleic acid-treated calcium carbonate (C3) in TPS3 exhibited large agglomerates, unlike TPS1, which used untreated calcium carbonate (C1). The large agglomerates of oleic acid-treated calcium carbonate filler created visible voids in TPS3, reducing its hardness compared to TPS1. Acid-treated composites (TPS1 and TPS3) displayed noticeable porosity, with irregular cavities resulting from the partial dissolution of calcium carbonate by citric acid. TPS3 showed larger dents, corresponding to the agglomerates, while TPS1 had smaller, more uniform cavities. These SEM observations confirm that the oleic acid-treated filler and increased porosity in TPS3 contributed to the material's weaker structure but improved liquid adsorption.

The surface roughness of the materials was analyzed using 3D images from the SEM micrographs (Fig. 5b), and the roughness parameters are shown in Table 2. Oleic acid and citric acid treatments influenced these properties. Untreated PS (NPS1) had a smooth surface with low roughness (RMS: 95.1673 nm, Sa: 71.5328 nm), indicating a uniform surface. In untreated composites (NPS1 and NPS3), roughness increased due to filler content and subsequent particle agglomeration in NPS3,

which showed the highest RMS (294.5760 nm) and Sa (255.2710 nm). This agrees with the observation by Hayeemasae et al. that an increased calcium carbonate content enhances a composite's tensile strength [35] (Hayeemasae & Ismail, 2021). As the oleic acid concentration increased, agglomeration intensified, creating a rough surface with noticeable peaks. Citric acid treatment caused a slight increase in roughness in pure PS, likely due to surface artifacts. In contrast, citric acid-treated composites (TPS1 and TPS3) had lower surface roughness than untreated ones, as citric acid dissolved some calcium carbonate, creating a porous structure and reducing roughness, promoting wettability and solvent adsorption.

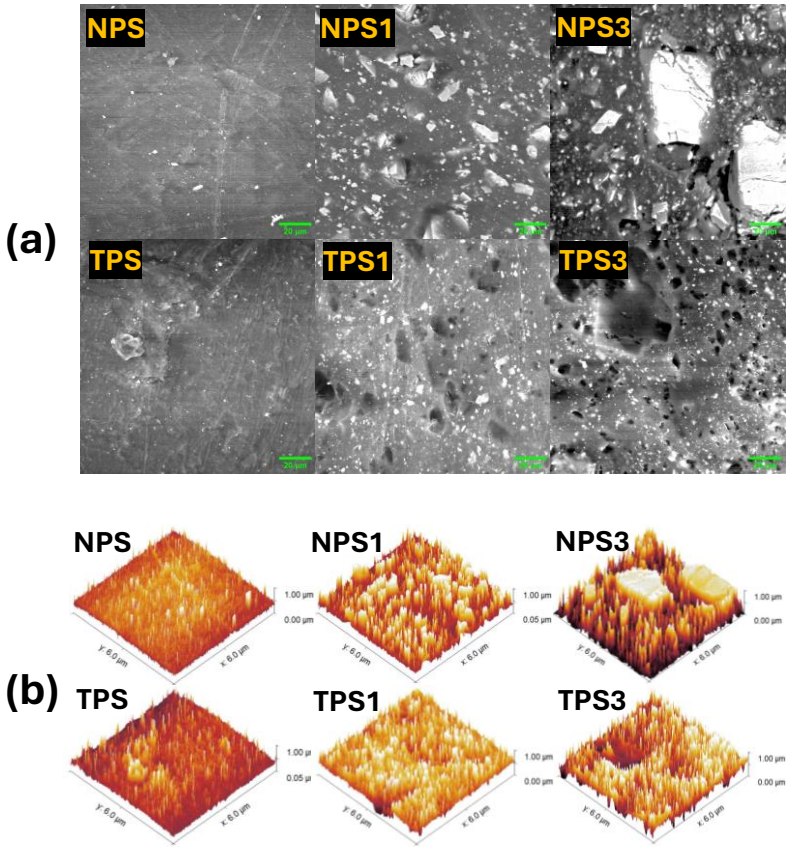

Fig. 5. SEM images showing the surface morphology of the polystyrene composites (a) and surface roughness profiles comparing polystyrene and polystyrene composites (b).

Table 2. Roughness parameters of the polystyrene and polystyrene composites.

Sample	RMS Roughness (Sq)	Mean Roughness (Sa)	Maximum Peak Height (Sp)	Maximum Pit Depth (Sv)
NPS	95.1673 nm	71.5328 nm	0.5145 µm	0.4815 µm
TPS	98.8757 nm	71.9033 nm	0.5654 µm	0.3796 µm
NPS	151.8080 nm	109.1970 nm	0.5238 µm	0.4291 µm
TPS1	132.5170 nm	93.6770 nm	0.4272 µm	0.5727 µm
NPS3	294.5760 nm	255.2710 nm	0.6630 µm	0.3369 µm
TPS3	197.4100 nm	150.8040 nm	0.5469 µm	0.4530 µm

Photoluminescence

The emission spectra (Fig. 6a(i) and 6b(i)) and CIE chromaticity diagrams (Fig. 6a(ii) and 6b(ii)), recorded at 255 nm and 405 nm excitation wavelengths, reveal the effects of oleic acid and citric acid treatments on the fillers and composites. The broad emission peaks observed are consistent with previous studies on polymeric materials [36-38]. Interestingly, as the excitation wavelength was increased, the emission peaks exhibited both a shift and a narrowing, indicating a wavelength-dependent luminescent response [38]. At 255 nm excitation, all samples showed broad emission peaks centered around 406 nm, with TPS composites displaying the broadest curves, even wider than NPS composites. Citric acid-treated composites (TPS1, TPS2, TPS3) exhibited narrower emission peaks

and a shift to lower wavelengths compared to their counterparts (NPS1, NPS2, NPS3), indicating that oleic acid treatment reduced defect-related emissions. In contrast, citric acid treatment introduces defect states, broadening the emission and causing a red shift. At 405 nm excitation, the emission peaks were centered around 570 nm, with pure NPS showing the lowest intensity, slightly below pure TPS. NPS3 displayed the highest intensity, while the citric acid-treated TPS composites exhibited intermediate intensities and a slight shift toward longer wavelengths compared to the NPS composites. These findings suggest that oleic acid treatment enhances light emission intensity and shifts the color to shorter wavelengths. In contrast, citric acid treatment introduces defects that reduce intensity and shift the color to longer wavelengths. CIE color maps (Fig. 6a(ii) and 6b(ii)) show a cluster in the blue-violet region under 255 nm excitation, shifting towards yellow-green under 405 nm excitation. Additionally, NPS3 and TPS3 demonstrated remarkable photoluminescent stability after 10 cycles of excitation and relaxation at 255 nm (Figures 7a and 7b), highlighting the tunability and stability of the composites' photoluminescent properties. Oleic acid treatment improves luminescence at lower concentrations, while citric acid treatment stabilizes radiative transitions and enhances photoluminescence, offering a tunable approach to modifying the optical properties of these materials.

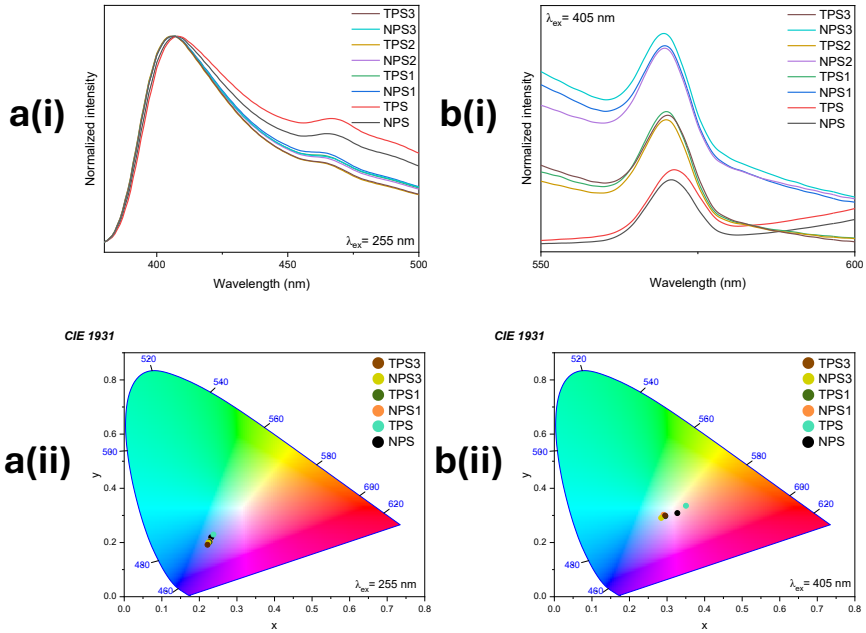

Fig. 6. Photoluminescence emission spectra at excitation wavelengths of 255 nm (a(i)) and 405 nm (b(i)), along with CIE color map spectra for 255 nm (a(ii)) and 405 nm (b(ii)).

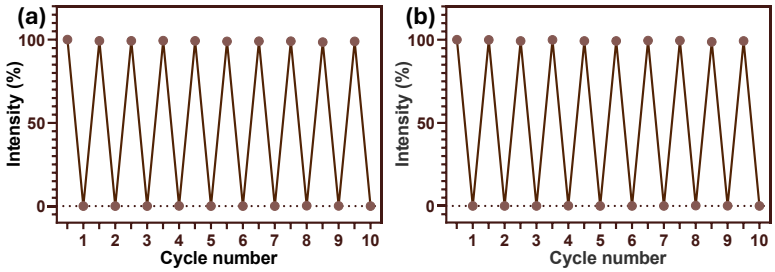

Fig. 7. Photoluminescence stability of (a) NPS3 and (b) TPS3 after 10 cycles of excitation and relaxation at 255 nm.

Shore Hardness Results

The Shore hardness values in Fig. 8a show changes due to the incorporation of composites, reflecting their mechanical performance. Untreated and treated PS (NPS and TPS) had a hardness of 78.30, while the addition of carbonate fillers initially increased hardness, peaking in NPS1 and TPS1, then declining with higher oleic acid treatment in NPS3 and TPS3. The decline in hardness was attributed to surface modifications that induced agglomeration and porosity. Toro et al. and

Hayeemasae et al. found that the increased particle size of eggshell fillers in PS composites led to reduced tensile strength [35]**.** The ANOVA results show a significant difference among the means ($F = 269.0$, $P < 0.0001$), with a strong model fit (R-squared = 0.9916). Dunnett's test revealed significant differences in hardness for all treatments, while the low residual variance ($P = 0.8469$) indicates minimal error in the data. This decline can be attributed to the dual effects of surface modifications and porosity introduced during oleic acid and citric acid treatments. This observed softening was attributed to the formation of agglomerates after the oleic acid treatment, which reduces its bonding strength within the polymer matrix. The citric acid treatment, on the other hand, dissolved portions of the calcium carbonate, creating pores that softened the composite structure. These two factors contributed to the decline in the hardness.

Solvent Affinity Test

The graph in Fig. 8b presents the weight gain percentage of the materials when immersed in water, vegetable oil, hexane, and diesel. Samples NPS and TPS showed minimal weight gain compared to the other composites, indicating low porosity and poor absorption capacity. In contrast, citric acid-treated composites (TPS1–TPS3) demonstrated a marked increase in absorption for the solvents, which aligns with the increased porosity, which increased the surface area available for absorption and the composite's modified surface, which increased hydrophobicity. The highest weight gain is observed in TPS3. Interestingly, water absorption remains relatively low across all samples, underscoring the hydrophobic nature of the treated composites due to the matrix. Treated composites traded some hardness for better absorption, and they have displayed a preference for non-polar solvents.

The ANOVA statistical analysis presented in Table 3 confirms that both the solvent and sample materials significantly influence adsorption, with very low P-values (< 0.0001) and high F-values (4067.40 for solvent and 3294.97 for sample materials). The interaction between solvent and sample materials also plays a significant role ($F = 206.46$, $P < 0.0001$), accounting for 10.93 % of the total variance. This suggests that both factors have a major impact on absorption and interact in a way that depends on the material type. Dunnett's multiple comparisons test further highlighted significant differences in absorption for all treatments compared to water, reinforcing the robustness and statistical significance of the results ($P < 0.0001$). The results show that both the type of solvent and the materials being tested strongly influence how much they absorb, with both factors having a very big impact. Additionally, the way the solvent interacts with the materials changes depending on the material type, making their combined effect significant. This means that neither the solvent nor the material behaves the same across all conditions, which is important when predicting performance in real-world applications.

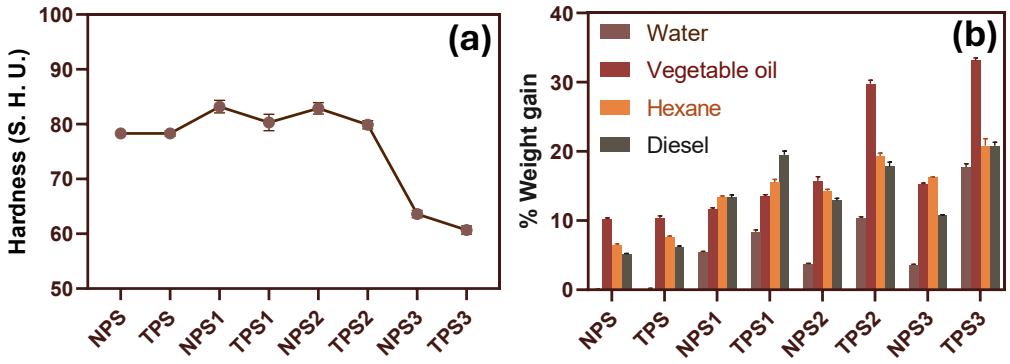

Fig. 8. (a) Hardness measurements of the composites, and (b) solvent absorption capacity.

Table 3. ANOVA analysis summary for the solvent affinity test.

Source of Variation	Degrees of Freedom (DF)	Sum of Squares (SS)	Mean Square (MS)	F Value	P Value	Variance Contribution (%)
Solvent	3	1623	541.0	4067.40	< 0.0001	30.76
Sample Materials	7	3068	438.3	3294.97	< 0.0001	58.15
Interaction	21	576.7	27.46	206.46	< 0.0001	10.93
Residual (Error)	64	8.513	0.1330	-	-	0.16
Total	95	5276	-	-	-	100.00

Conclusion

This study investigated the impact of oleic acid and citric acid treatments on the properties of PS-calcium carbonate composites, focusing on hydrophobicity, morphology, photoluminescence, hardness, and solvent adsorption. The carbonate fillers were treated with various concentrations of oleic acid before being incorporated into the polymer matrix via melt blending. The resulting composites were subsequently treated with citric acid. Key findings indicate that oleic acid treatment enhanced hydrophobicity but reduced surface hardness, whereas citric acid treatment increased porosity through calcium carbonate dissolution. XRD and FTIR analyses confirmed the presence of all composite components, with no evidence of chemical bonding between the filler and polymer matrix. SEM images revealed that higher concentrations of oleic acid led to filler agglomeration, while citric acid treatment increased surface roughness and porosity. Photoluminescence spectra revealed that oleic acid treatment narrowed emission peaks, enhancing luminescence, whereas citric acid induced defect states, leading to emission shifts. Shore hardness measurements indicated a reduction from 83.20 to 60.70, while solvent absorption tests demonstrated a trade-off between mechanical properties and absorption capacity, with vegetable oil exhibiting the highest absorption (33.10%). Overall, oleic acid treatment improved hydrophobicity and photoluminescence, while citric acid treatment primarily contributed to porosity and hydrophilicity. These findings demonstrate that oleic acid and citric acid treatments provide a tunable strategy for modifying PS-calcium carbonate composites, enhancing their potential for adsorption and smart pollutant detection applications.

Acknowledgments

Ayodunmomi Esther Olowofoyeku sincerely thanks the African Union and the Pan African University Life and Earth Sciences Institute for awarding a Ph.D. scholarship for this research as a part of her doctoral research.

References

[1] E. Awodi, and K. Adewumi, Exploring the Aesthetic Applications of Expanded Polystyrene: An Interdisciplinary Review, AJIMS 6 (2024) 1-15.

[2] R. Yadav, M. Singh, D. Shekhawat, S.-Y. Lee, and S.-J. Park, The role of fillers to enhance the mechanical, thermal, and wear characteristics of polymer composite materials: A review, Compos. - A: Appl. Sci. Manuf. 175 (2023) 1-9.

[3] Z. Ali, S. Yaqoob, J. Yu, and A. D'Amore, Critical review on the characterization, preparation, and enhanced mechanical, thermal, and electrical properties of carbon nanotubes and their hybrid filler polymer composites for various applications, Compos. C: Open Access 13 (2024) 1-11.

[4] R. He, Y. Wu, Y. Liu, L. Luo, H. Xiao, C. Huang, X. Wang, Z. Zeng, J. He, and Y. Zhang, A superhydrophilic/air superoleophobic sponge based on low-temperature vacuum evaporation deposition modification for saving marine crude oil pollution and leakage, Prog. Org. Coat. 188 (2024) 1-13.

[5] M.O. Awan, A. Shakoor, M.S. Rehan, and Y.Q. Gill, Development of HDPE composites with improved mechanical properties using calcium carbonate and NanoClay, Phys. B: Condens. Matter. 606 (2021) 1-16.

[6] A.H. Ritonga, N. Jamarun, S. Arief, H. Aziz, D.A. Tanjung, and B. Isfa, Improvement of Mechanical, Thermal, and Morphological Properties of Organo-Precipitated Calcium Carbonate Filled LLDPE/Cyclic Natural Rubber Composites, Indones. J Chem. 22 (2022) 233-241.

[7] F.C. Chiu, S.M. Lai, C.M. Wong, and C. Hui Chang, Properties of calcium carbonate filled and unfilled polystyrene foams prepared using supercritical carbon dioxide, J. Appl. Polym. Sci. 102 (2006) 2276-2284.

[8] E. Wang, L. Xiang, B. Tang, X. Dai, Z. Cao, T. Jiang, Y. Wang, X. Chen, W. Li, Y. Zhao, K. Yang, and X. Wu, Preparation and Compression Resistance of Lightweight Concrete Filled with Lightweight Calcium Carbonate Reinforced Expanded Polystyrene Foam, Polymers 15 (2023) 1-11.

[9] A. Homavand, D.E. Cree, and L.D. Wilson, Polylactic Acid Composites Reinforced with Eggshell/CaCO3 Filler Particles: A Review, Waste 2 (2024) 169-185.

[10] N. Mahmood, and M. Hikmat, The Effect of Calcium Carbonate-Nanoparticle on the Mechanical and Thermal Properties of Polymers Utilizing Different Types of Mixing and Surface Pre-Treatment: A Review Paper, J. Eng. Technol. (2023) 1-19.

[11] J. Qiu, J.W. Lyu, J.L. Yang, K.B. Cui, H.Z. Liu, G.F. Wang, and X. Liu, Review on Preparation, Modification and Application of Nano-Calcium Carbonate, Part. Part. Syst. Charact. 41 (2024) 1-12.

[12] A. Patti, H. Lecocq, A. Serghei, D. Acierno, and P. Cassagnau, The universal usefulness of stearic acid as surface modifier: applications to the polymer formulations and composite processing, J. Ind. Eng. Chem. 96 (2021) 1-33.

[13] R. Dweiri, Processing and Characterization of Surface Treated Chicken Eggshell and Calcium Carbonate Particles Filled High-Density Polyethylene Composites, Mater. Res. 24 (2021).

[14] L.T. Wang, Q. Chen, R.Y. Hong, and M.R. Kumar, Preparation of oleic acid modified multi-walled carbon nanotubes for polystyrene matrix and enhanced properties by solution blending, J. Mater. Sci.: Mater. Electron. 26 (2015) 1-9.

[15] N.M.F. Hakimi, S.H. Lee, W.C. Lum, S.F. Mohamad, S.S. Osman Al Edrus, B.-D. Park, and A. Azmi, Surface Modified Nanocellulose and Its Reinforcement in Natural Rubber Matrix Nanocomposites: A Review, Polymers 13 (2021) 1-24.

[16] A. Kawamura, M. Saijyo, B. Bayarkhuu, N. Nishidate, I. Oikawa, S. Kobayashi, K. Oyanagi, Y. Shiba, T. Tsukamoto, Y. Oishi, and Y. Shibasaki, Fabrication of hyperbranched-polyglycidol-Fe_3O_4 nanocomposite labeled with fluorescein isothiocyanate via rapid ligand exchange reaction, Polymer 294 (2024) 1-10.

[17] N.H. Aprilita, T. Febriani, P. Ofens, M. Nora, T.A. Nassir, E.T. Wahyuni, N. Sciences, and U.G. Mada, Conversion of the styrofoam waste into a high-capacity and recoverable adsorbent in the removing the toxic Pb^{2+} from water media, 26 (2024) 1-10.

[18] I. Dragutan, F. Ding, Y. Sun, and V. Dragutan, Recent Developments in Multifunctional Coordination Polymers, Crystals 14 (2024) 1-7.

[19] P. Chenna, S. Gandi, S. Pookatt, and S.R. Parne, Perovskite white light emitting diodes: A review, Mater. Today Electron. 5 (2023) 1-24.

[20] P. Melnikov, A. Bobrov, and Y. Marfin, On the Use of Polymer-Based Composites for the Creation of Optical Sensors: A Review, Polymers 14 (2022) 1-36.

[21] A.K. Singh, Multifunctionality of lanthanide-based luminescent hybrid materials, Coord. Chem. Rev. 455 (2022) 1-9.

[22] A.H. Ritonga, N. Jamarun, S. Arief, H. Aziz, D.A. Tanjung, B. Isfa, V. Sisca, and H. Faisal, Organic modification of precipitated calcium carbonate nanoparticles as filler in LLDPE/CNR blends with the presence of coupling agents: impact strength, thermal, and morphology, J. Mater. Res. Technol. 17 (2022) 2326-2332.

[23] N. Thyashan, Y.S. Perera, R. Xiao, and C. Abeykoon, Investigation of the effect of materials and processing conditions in twin-screw extrusion, Int. J. Lightweight Mater. Manuf. 7 (2024) 353-361.

[24] H.M. Abd El-Lateef, M.M. Khalaf, M.F. Abou Taleb, and M. Gouda, Development of photoluminescent concrete from polystyrene plastic reinforced with electrospun polypropylene nanofibers, J. Photochem. Photobiol. A: Chem. 449 (2024) 1-9.

[25] M. Al-Shirawi, M. Karimi, and R.S. Al-Maamari, Impact of carbonate surface mineralogy on wettability alteration using stearic acid, J. Pet. Sci. Eng. 203 (2021) 1-11.

[26] P.M. Claesson, N.A. Wojas, R. Corkery, A. Dedinaite, J. Schoelkopf, and E. Tyrode, The dynamic nature of natural and fatty acid modified calcite surfaces, Phys. Chem. Chem. Phys. 26 (2024) 2780-2805.

[27] N.A.M. Nasir, W.M.I.W.M. Kamaruzzaman, M.A. Badruddin, and M.S. Mohd Ghazali, Surface modification effects of $CaCO_3$ and TiO_2 nanoparticles in nonpolar solvents, J. Dispersion Sci. Technol. 45 (2024) 870-879.

[28] Y. Ma, P. Tian, M. Bounmyxay, Y. Zeng, and N. Wang, Calcium Carbonate@silica Composite with Superhydrophobic Properties, Molecules 26 (2021) 1-14.

[29] B. Kirkebæk, G. Simoni, I. Lankveld, M. Poulsen, M. Christensen, C.A. Quist-Jensen, D. Yu, and A. Ali, Oleic acid-coated magnetic particles for removal of oil from produced water, J. Pet. Sci. Eng. 211 (2022) 110088-110088.

[30] A.A. Al-Muntaser, R.A. Pashameah, E. Alzahrani, S.A. AlSubhi, and A.E. Tarabiah, Tuning structural, optical, and dispersion functions of polystyrene via addition of meso-tetraphenylporphine manganese (III) chloride towards optoelectronic applications, Opt. Mater. 135 (2023) 1-12.

[31] R. de Sousa Cunha, G.D. Mumbach, R.A.F. Machado, and A. Bolzan, A comprehensive investigation of waste expanded polystyrene recycling by dissolution technique combined with nanoprecipitation, Environ. Nanotechnol. Monit. Manag. 16 (2021) 1-7.

[32] P. Zapata, H. Palza, B. Díaz, A. Armijo, F. Sepúlveda, J. Ortiz, M. Ramírez, and C. Oyarzún, Effect of $CaCO_3$ Nanoparticles on the Mechanical and Photo-Degradation Properties of LDPE, Molecules 24 (2018) 1-12.

[33] H.E. Benchouia, H. Boussehel, B. Guerira, L. Sedira, C. Tedeschi, H.E. Becha, and M. Cucchi, An experimental evaluation of a hybrid bio-composite based on date palm petiole fibers, expanded polystyrene waste, and gypsum plaster as a sustainable insulating building material, Constr. Build. Mater. 422 (2024) 1-10.

[34] A. Bhattacharya, and S.K. Khare, Bioinspired mineralization and remediation of polystyrene nanoparticles by urease-induced calcite precipitation, J. Environ. Chem. Eng. 12 (2024) 1-10.

[35] N. Hayeemasae, and H. Ismail, Potential of calcium carbonate as secondary filler in eggshell powder filled recycled polystyrene composites, Polímeros 31 (2021) 1-7.

[36] M. Gouda, H.M. Abd El-Lateef, M.F. Abou Taleb, and M.M. Khalaf, Photoluminescent polypropylene nanofiber-supported polyethylene terephthalate integrated with strontium aluminate phosphor, J. Photochem. Photobiol. A: Chem. 453 (2024) 1-9.

[37] M. Gouda, H.M. Abd El-Lateef, M.F. Abou Taleb, and M.M. Khalaf, Polylactic acid film embedded with phosphor nanoparticles: Photochromic and afterglow biodegradable window and concrete, J. Mol. Struct. 1300 (2024) 1-10.

[38] M. Tareeva, M. Shevchenko, S. Umanskaya, V. Savichev, A. Baranov, N. Tcherniega, and A. Kudryavtseva, Two-Photon Excited Luminescence in Polyethylene and Polytetrafluoroethylene, J. Russ. Laser Res. 41 (2020) 502-508.